Copenhagen '12

Y019

Constraining the Petro-elastic Model with a Flatlander's Interpretation of the 4D Signal

E. Alvarez* (Heriot-Watt University) & C. MacBeth (Heriot-Watt University)

SUMMARY

An analytic formulation is obtained that relates mapped time-lapsed seismic amplitudes and time-delays directly to the sum of reservoir pressure and saturation changes weighted by the principal groups of controlling parameters from the petroelastic model. Application to data from the North Sea and West Africa provides insight into how the petroelastic model controls the seismic response and the relative interplay between pressure and saturation changes for each reservoir type. These data, together with published literature examples, allow the identification of regions in the reservoir where the saturation-driven 4D signature dominates over the pressure-driven, or vice-versa. These observations are used to determine a simple constraint on the relative magnitude of the controlling groups of petroelastic model parameters. It is concluded that the evaluation of 4D seismic as saturation- or pressure-dominated is a key measurement for our understanding of the in situ petroelastic model.

Introduction

Past work on 4D seismic interpretation has shown how pressure and saturation changes may affect mapped time-lapse seismic amplitudes. For example, Landrø (2001) developed expressions for the AVO behaviour of the top reservoir interface. In a development suited to a generalized range of attributes and independent of the petroelastic model, MacBeth et al. (2006) suggested an expression that is linear in pressure and saturation change, with weights determined from the correlation between the 4D seismic data and the well production data. Unfortunately, neither of these techniques is immediately useful for revealing the direct impact of the petroelastic model on the 4D seismic signatures, without recourse to a full calculation. Additionally, it would be useful to be able to explicitly identify lateral variations in the 4D seismic signature with key reservoir properties such as porosity, fluid contrast, fluid compressibility or rock frame stress sensitivity. These objectives are addressed in the current work and considered for the case of clastic reservoirs for which the predominant changes are due only to fluid pressure, or oil and water movement.

Theory and method

Consider a single plane horizontal interface representing the contrast between a producing reservoir and an overlying inert shale. No variations with net-to-gross or reservoir thickness are treated in this current work, and only a single interface is considered. Our starting point is the Gray et al. (1999) first order, weak contrast approximation to the Zoeppritz equations, which gives the reflection coefficient as a function of incidence angle θ in terms of bulk modulus κ, shear modulus μ, density ρ

$$R(\theta) = \left(\frac{1}{4} - \frac{1}{3}\left(\frac{\overline{V_S}}{\overline{V_P}}\right)^2 \right) \Gamma_1 \frac{\Delta\kappa}{\overline{\kappa}} + \left(\frac{\overline{V_S}}{\overline{V_P}}\right)^2 \Gamma_2 \frac{\Delta\mu}{\overline{\mu}} + \Gamma_3 \frac{\Delta\rho}{\overline{\rho}}. \quad (1)$$

Here, the operator Δ refers to a difference of that particular property across the interface and the over-score to an average of the properties either side of the interface. The equation is also controlled by the weighting of the average shear to P-wave velocity ratio at the interfaces $(\overline{V}_S / \overline{V}_P)$.The angular dependence is captured in the terms $\Gamma_1=\sec^2\theta$, $\Gamma_2=(1/3)\sec^2\theta - 2\sin^2\theta$, and $\Gamma_3=(1/2)-(1/4)\sec^2\theta$.
Now consider the application of (1) to a reservoir that is imaged before, and then during, its lifetime of production and recovery. By introducing the petroelastic model and following MacBeth et al. (2006), the changes in the elastic moduli above are written in terms of first order perturbations in pressure ΔP and saturation ΔS_w and the parameters of the petroelastic model itself. The time-lapsed change in the reflection coefficient ΔR_{TL} between the monitor and the pre-production (baseline) survey time is given by

$$\overline{\Delta R}_{TL} = \phi\left[\overline{\Gamma}_1 N_1 + \overline{\Gamma}_2 N_2\right]\Delta S_W - \left\{(1-\varepsilon'\phi)\left[\overline{\Gamma}_1 N_3 + \overline{\Gamma}_3 N_4\right] - \phi\left[\overline{\Gamma}_1 N_5 + \overline{\Gamma}_2 N_6\right]\right\}\Delta P \quad (2)$$

where $\overline{\Gamma}_1$, $\overline{\Gamma}_2$, and $\overline{\Gamma}_3$ are now averages over the functions of incidence angle, ϕ the reservoir porosity and ε' a material constant. Each of the *N*-constants has a direct physical interpretation: N_1 relates to the contrast in bulk modulus between water (the displacing fluid) and the mobile oil, N_2 is the corresponding density contrast, N_3 and N_4 define the rock stress sensitivity (both the bulk and shear modulus parts), and finally N_5 and N_6 represent the impact of pressure changes on the fluid bulk modulus and density. Of importance to note here is that these petroelastic parameters act together as a single lumped coefficient, and thus they may be regarded as inseparable in terms of their influence on the seismic data. The accuracy of (2) is tested against full numerical computation, and for pressure changes in the range -5MPa to +5MPa, and water saturation changes in the range +20% to 80% appropriate for our reservoir of interest, with errors remaining at less than 2.5%. A comparison of (2) with full simulator to seismic modelling (Amini and MacBeth, 2011) also further validates the approach, with normalised errors in the maps of less than 3% (Figure 1).

The parameterisation in (2) captures in quantitative form much about the time-lapse seismic signature

that is already well understood intuitively. The equation provides a way of identifying how individual reservoir conditions affect the petroelastic model, and in turn how this might control and modify the resultant mapped seismic response. Interestingly, the dependence on porosity is now captured explicitly and it is seen how the time-lapse seismic signature scales with this parameter. The saturation term is controlled by a group of parameters which scale directly with the contrast between the water and oil bulk moduli and densities. On the pressure side of the equation, there are two competing parameter groups: the first relates to the magnitude of rock frame stress sensitivity and the second to the variation of the bulk modulus and density of the fluids. The equation shows that these last two terms must compete against each other.

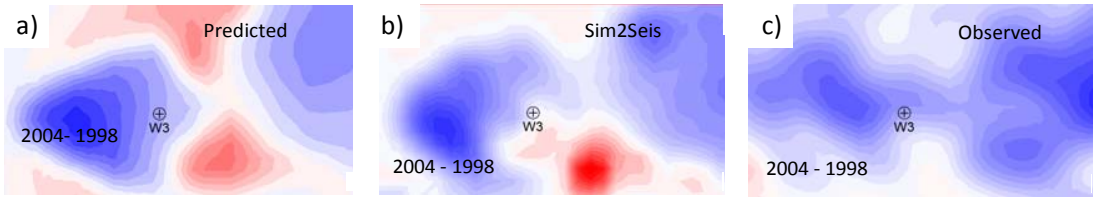

Figure 1 *Mapped seismic amplitude for a North Sea reservoir predicted from pressure and saturation changes obtained from the simulation model. (a) Predictions based on the approximate equation (2); (b) simulator to seismic calculation; (c) Observed 4D seismic response.*

4D seismic interpretation

In practice, the observed time-lapse seismic amplitude is the change in the stacked (and migrated) response for a specific range of offsets, and is estimated within a time-window defined across a particular reservoir event (usually top reservoir). The reflection coefficient ΔR_{TL} is thus scaled by a wavelet function, and should now be replaced by the amplitude ΔA_{TL}. For the purposes of the current work it is assumed that the requisite scaling factor has been absorbed into the *N*-coefficients that multiply both the pressure and saturation changes in (2). Simplifying, the seismic amplitudes can now be written in the compact form

$$\Delta A_{TL} = C_S \Delta S_w - C_P \Delta P \tag{3}$$

where the two controlling parameters C_S and C_P relate directly to the fundamental constants *N1* to *N6* and to porosity. A negative sign is preserved in (3) so that regardless of whether the impedance contrast at the event of interest is low to high, or high to low, the coefficients C_S and C_P remain positive. This also makes sense as an increase in saturation (hardening of impedance) has an opposing physical effect on the reservoir to an increase in pressure (softening of impedance).

Observed seismic data examples

Equation (3) interprets 4D seismic amplitudes as a weighted combination of pressure and saturation change, and selected seismic observations can be used to back out the relative magnitudes of C_S and C_P in situ (as defined by the ratio C_S/C_P). Here, it is observed that the basic measurement of a 4D signature as being dominated by either saturation or pressure provides a simple and obvious way to determine this constraint from the seismic data. However, only situations in which pressure and water saturation increase can be considered, as $C_S\Delta S_w$ then competes against $C_P\Delta P$ in the determination of data polarity and overall dominance of the signal. This condition restricts our measurements to regions of the reservoir for which water is injected. Observed 4D seismic data from a North Sea clastic reservoir are analysed initially (Figure 2). Stacked and migrated seismic data are available for the 1998 (pre-productionbaseline) and the 2004, 2006 and 2008 post-production monitor surveys. The flow simulation model is also available and the injector wells (W1 and W2) are chosen because the production history match in the selected areas is good. Simulation results for the period 1998 to 2004 show a pressure change of +3.5MPa around W2, but less than +0.5MPa around W1 due to de-

pressurisation effects. Both wells have a similar saturation change during this period, this being +0.45 and +0.44 respectively. There is no gas in the area and it is known that an increase in the observed amplitudes indicates pressure up in the reservoir, whilst a decrease in the amplitudes reveals an influx of water. The observed 4D seismic (2004-1998) shows a RMS mapped amplitude increase at W1, consistent with saturation effects dominating, this giving the relation $0.45C_S > 0.5C_P$. At W2, the seismic indicates only a small RMS mapped amplitude decrease signal consistent with a pressure increase. Thus, it looks like the saturation and pressure changes partially cancel around this well, and $0.44C_S \approx 3.5C_P$.

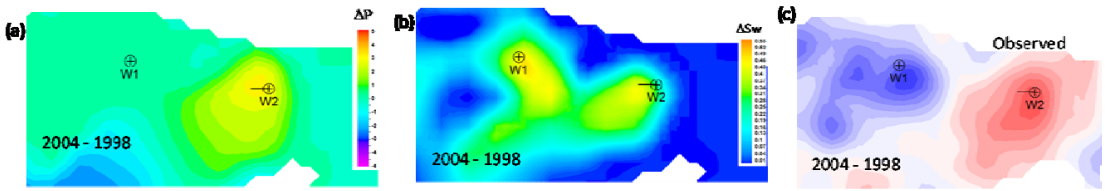

Figure 2 *(a) Pressure and (b) saturation changes for our initial field example predicted from the simulation model. (c) Observed 4D seismic response (2004 to 1998 surveys only).*

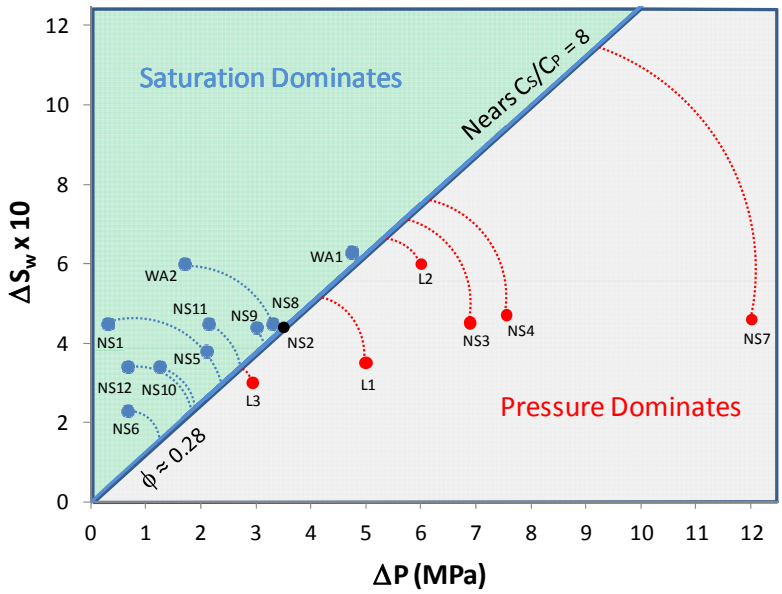

Figure 3 *Colour coding according to whether the 4D signatures are dominated by saturation (blue) or pressure (red). The line $C_S/C_P=8$ is drawn as the best fit boundary between the saturation and pressure dominant domains. Points are taken from a North Sea dataset (NS1 to NS12), West Africa dataset (WA1 to WA2), and several literature examples (L1 to L3). The circular arcs represent inequalities.*

The C_S-C_P data are brought together in Figure 3, which plots $10\Delta Sw$ against ΔP to ensure the points or inequalities fall in a central location on the plot. The observations above contribute points NS1 and NS2. Further points are added to this plot by the remaining monitor survey data (points NS3 to NS12), two West Africa examples (points WA1 and WA2), and gathered literature examples (Johann et al. 2009, Floricich, 2006, and Landrø, 2001) (points L1, L2 and L3).

Discussion

In Figure 3, the boundary that divides the two regimes of pressure and saturation dominance is delineated by a straight line with a slope C_S/C_P, this depending on the reservoir's petroelastic model parameters and the porosity. It is found that the observation points for our data can be divided by a line with slope $C_S/C_P = 8$. Numerical calculation of this ratio using the known petroelastic parameters, and the porosities for our North Sea reservoir conclude that it should lie between 5 and 10. Note that if reservoir porosity is low, it is anticipated that C_S/C_P will be higher than 8. However, no low porosity examples exist in the literature to date to verify this prediction. The above result has implications for the underlying petroelastic model used to characterise the rock and fluid physics. In particular, from (2) this constraint provides a way of linking the fluid contrast between the original and displaced fluids, and the largely uncertain rock stress sensitivity. This is possible, as the fluid contrast terms are relatively well known functions of the bulk modulus and density of the oil and brine, and the initial water saturation. For a mean porosity of 25%, and oil-water displacement for the reservoirs in our North Sea example, we obtain the constraint

$$0.25N_3 + 0.33N_4 \approx 0.015 \tag{4}$$

where *N3* and *N4* are defined as dependent variables of the stress sensitivity functions for κ and μ. This equation is a means of constraining possible stress sensitivity curves extracted from the laboratory or from theory. It is a useful tool for selecting those solutions acceptable to both the seismic and appropriate laboratory measurement.

Conclusions

A formulation has been obtained that predicts the relative contributions of pressure and saturation change to the time-lapsed seismic amplitudes, and brings out the explicit role of the petroelastic model parameters. It is found that porosity plays an important controlling role, and so too does the initial saturation state. It is expected for porosities larger than 20%, saturation will dominate in most reservoirs, whilst for porosities smaller than 20%, then pressure dominates. The results of this study suggest that C_S/C_P is a fundamental parameter that can be unambiguously extracted from the 4D seismic amplitudes by observing whether saturation or pressure dominates the response at a select number of injector locations. Further, according to the data collected from five clastic reservoirs, $C_S/C_P = 8$ seems to indicate the point at which pressure dominates over saturation, and vice-versa.

Acknowledgements

We thank the sponsors of the Edinburgh Time Lapse Project, Phase IV, for their support (BG, BP, Chevron, ConocoPhillips, ENI, ExxonMobil, Hess, Ikon Science, Landmark, Maersk, Marathon, Norsar, RSI, Petrobras, Shell, Statoil, and Total). Schlumberger are thanked for providing Petrel and Eclipse software. EA thanks Hamed Amini for his contribution to this work, and also acknowledges financial support from Senergy (GB).

References

Amini, H., MacBeth, C. [2011] Calibration of simulator to seismic modelling for quantitative 4D seismic interpretation. 73rd EAGE Conference & Exhibition incorporating SPE EUROPEC 2011

Floricich, M. [2006] An engineering-consistent approach for pressure and saturation estimation from time-lapse seismic data, PhD thesis, Heriot-Watt University

Gray, D., Goodway, B., Chen, T. [1999] Bridging the Gap: Using AVO to detect changes in fundamental elastic constants. SEG Expanded Abstracts 18, 852-855

Johann, P., Sansonowski, R., Oliveira, R. and Bampi, D. [2009] 4D seismic in a heavy-oil, turbidite reservoir offshore Brazil. The Leading Edge 28, 718-729

Landrø, M. [2001] Discrimination between pressure and fluid saturation changes from time-lapse seismic data. Geophysics, 66, 836–844

MacBeth, C., Floricich, M. and Soldo, J., 2006, Going quantitative with 4D seismic analysis:

Geophysical Prospecting, 54, 303-318